

Geostatistical analysis and spatial distribution map of geochemical contents of the Susuzdag Formation limestones

Susuzdag Formasyonu kireçtaşlarının jeokimyasal içeriklerinin jeoistatistiksel analizi ve mekânsal dağılım haritası

Ozge OZER ATAOKLU^{1*} , Mustafa Gurhan YALCIN² 

^{1,2}Dep. of Geological Engineering, Mineral Deposits and Geochemistry, Faculty of Engineering, Akdeniz University, Antalya, Turkey.,
oozer@akdeniz.edu.tr, guruhanyalcin@akdeniz.edu.tr

Received/Geliş Tarihi: 20.04.2021

Revision/Düzeltilme Tarihi: 23.08.2021

doi: 10.5505/pajes.2021.82609

Accepted/Kabul Tarihi: 24.08.2021

Research Article/Araştırma Makalesi

Abstract

Limestones, which are a type of carbonate rocks that are classified as karstification of rocks, are widely observed in the Antalya complex. The assessment of the elemental relationships in the formation of limestones by using statistical methods is important for the interpretation of paleo-redox states in the environment and for understanding its diagenetic conditions. In the study, limestone samples collected from the Susuzdag Formation were analyzed by the XRF method to determine their chemical contents. Also, thin cross-sections of the limestone samples were prepared and the mineralogical properties of the formation were determined by performing detailed optical microscopy examinations. The order of the contents enriched during the formation of limestones is as follows: SiO₂, MgO, Al₂O₃, K₂O, TiO₂, Fe₂O₃, SO₃, Pb, Th, U, Sr, Mn, and Co. The high values of K₂O, Al₂O₃ and SiO₂ elements at the regional scale revealed the high clay presence in the limestones. In addition, high concentrations of Al₂O₃ and TiO₂ interpreted from distribution maps in similar locations indicate the presence of minerals with aluminum oxide and titanium oxide. The cumulative value of chemical contents, which were observed to fall in 4 main groups, was calculated as 92.60%. The limestone samples were found to have micritic and sparitic textural features, and no foliation or lamination was observed in their thin cross-sections. Moreover, according to the single-nicol images, the matrix fillings of the cross-sections of the samples were found to contain clay. It was thought that the limestones in the region underwent dehydration reactions during their formation and lost their water molecules and became enriched in kaolinite minerals.

Keywords: Limestone, Multivariate statistics, Spatial statistics, Mineralogy, Geochemistry.

Öz

Karstlaşabilen kayaç sınıflamasına giren karbonatlı kayaçlardan kireçtaşları, Antalya kompleksi içerisinde yaygın olarak bulunurlar. Kireçtaşlarının oluşumunda meydana gelen elementel ilişkilerin istatistiksel metotlar kullanılarak yorumlanması, ortamdaki paleo-redoks durumlarının yorumlanması ve diyajenetik koşulların anlaşılabilmesi için önem arz etmektedir. Çalışmada, Susuzdag Formasyonu içerisinde bulunan kireçtaşlarından derlenen örnekler XRF yöntemiyle analiz edilmiştir. Ayrıca, kireçtaşı numunelerinden ince kesitler hazırlanmış olup ayrıntılı optik mikroskop çalışmaları ile formasyonun mineralojik özellikleri belirlenmiştir. Kireçtaşlarının oluşumu esnasında zenginleşme gösteren içeriklerin sıralanımı "SiO₂, MgO, Al₂O₃, K₂O, TiO₂, Fe₂O₃, SO₃, Pb, Th, U, Sr, Mn ve Co" şeklindedir. Bölgesel ölçekte K₂O, Al₂O₃ ve SiO₂ elementlerinin yüksek değerlerde bulunması, kireçtaşlarının içerisindeki yüksek kil varlığını ortaya çıkarmıştır. Ayrıca dağılım haritalarından yorumlanan Al₂O₃ ve TiO₂ benzer lokasyonlardaki yüksek konsantrasyonları alüminyumoksitli ve titanyumoksitli minerallerin varlığına işaret etmektedir. Başlıca 4 faktör altında toplandığı görülen kimyasal içeriklerin kümülatif değeri %92.60 olarak hesaplanmıştır. Mikritik ve sparitik dokusal özellikte bulunan kireçtaşlarının ince kesitlerinde foliasyon ve laminasyon gözlemlenmemiştir. Ayrıca kesitlerin matriks dolgularının kil içerikli olduğu tek nikol görüntülerinden tespit edilmiştir. Bölgedeki kireçtaşlarının oluşumları esnasında, dehidrasyon tepkimeleri geçirerek su moleküllerini kaybedip, kaolinit mineralince zenginleştikleri düşünülmüştür.

Anahtar kelimeler: Kireçtaşı, Çok değişkenli istatistik, Mekânsal istatistik, Mineraloji, Jeokimya.

1 Introduction

Limestones are carbonated units formed by karstification of rocks under suitable environmental conditions [1],[2]. Carbonate rocks are important with the rare earth elements and precious metals they contain [3]. These types of rocks are subject to dissolution under the influence of natural waters, allowing the formation of lithologies of different types and structures [4]. The formation of carbonate rocks does not depend solely on the calcium mineral. Also, carbonate rocks contain various minerals and elements in their content depending on their formation environment [5]. The physical environment conditions of the carbonate rocks affect their elemental composition. In the literature, there are several similar studies on determining the geological environmental conditions and elemental compositions of carbonate rocks.

In the study carried out on the limestone samples collected from northeast Iran, the mineral phases and elemental concentrations of the samples were determined. The results were evaluated using multivariate statistical methods, and information about the diagenetic conditions and processes that the limestones underwent was obtained. The mineralogical data obtained revealed that the major components of the limestones observed in the region were calcite and quartz while the minor contents were kaolinite and hematite minerals [3].

Geochemical investigations on limestone samples collected from the Kanigorgeh region in Iran facilitated making interpretations about the deposition environments of the limestones. It was concluded that the limestones observed in the region have been deposited under two different conditions. The metallic oxide enrichment that occurred with the adsorption of the kaolinite mineral in the environment has led

*Corresponding author/oozer@akdeniz.edu.tr

to the main formation mechanism of the limestones [6]. The study conducted on limestone samples collected from the Northern Ural region revealed details about the origin and mineralogical properties of carbonate facies. The mineralogical characteristic of the examined limestone samples was found to be microgranular calcite [7],[8].

Biogeochemical processes undergone by the carbonate rocks were investigated in studies on limestone samples collected from the Parnassos region of Greece. The presence of fossils was found in the limestone samples. Moreover, the presence of organic material has led to the development of bio-mineralization reactions. The limestone samples were found to have element enrichments due to various bioextraction reactions, and the correlations between the elements in limestones were determined [9].

The geochemical properties of the limestone samples collected from the South of the Seydisehir region in Central Anatolia were determined. The results of the chemical analyses of the carbonate rock formations in the region were evaluated using geochemical and geostatistical approaches. The limestone samples collected from the field were observed to have fossil content. Also, they were found to have medium to thick-bedded with a color scale between gray and cream in terms of their physical view. The results of the mineralogical investigations revealed that the main mineral content was dolomite. Also, it was determined that they showed dismicritic and intrapelmicritic textural features [10].

The study area, which is in the Western Taurides, is located in front of the Lycian Nappes in the East of Dalaman and Ortaca (Figure 1) [11].

The Sutlegen village is approximately 30 km inland from Kas harbor. The major units forming the geology of the region are as follows: Middle Eocene-Lower Miocene aged Elmali Formation, Middle Eocene-Lower Miocene Susuzdag Formation, and Quaternary aged alluvial material, which are the youngest units observed in the region. Most of the limestones in the region are observed in the Susuzdag Formation [12].

Although there are several studies highlighting the geological properties of the Western Taurides in the literature, no study has been conducted on the geochemical and mineralogical properties of neritic limestones observed in the Susuzdag Formation. In this context, the present study aims to examine the limestones in the region in terms of determining the chemical contents of the samples by analyzing them using XRF, interpreting the results of these analyses using multivariate statistical methods, generating spatial distribution maps of the results of the chemical analysis using Kriging interpolation method, and determining their textural and mineralogical features. It is also aimed to interpret the paleo-redox states, diagenetic conditions, and depositional environments of the limestones in the region.

2 Materials and methods

2.1 Geochemical analyses

A total of 35 limestone samples collected from the Sutlegen village were brought to the Geological Engineering Department of the Engineering Faculty at Akdeniz University. The samples were homogenized and ground to clay size (<10 µm) using the RM 200 mortar grinder (Retsch GmbH, Germany) to prepare for energy dispersive X-ray fluorescence (ED-XRF) chemical analysis [13],[14]. Then, the homogenized samples were taken to the hydraulic press machine to produce press-pastilles, and they were pressed under the pressure of 30MPa to have suitable dimensions for the XRF device [15]. The elemental spectra of the samples were created using a Rigaku NEX CG Energy Dispersive X-Ray Fluorescence (ED-XRF) spectrometer (NEX-CG Applied Rigaku Technologies, Inc. Austin, TX, USA) with an artificial X-ray tube of 50W and a fluorescence detector. The concentration values obtained from the spectra were calculated in ppm. Thus, the chemical composition of each sample was determined.

The samples collected from the field were brought to the Geological Engineering Department of the Faculty of Engineering Mines at Akdeniz University to analyze the mineralogical properties of the limestone samples. Five of the limestone samples were cut into small pieces using water. The samples were subjected to surface wearing and epoxy processes to examine them sensitively using an optical microscope and to determine their mineralogical contents. Then, the limestones (thin cross-sections) obtained from these processes were placed on the glass lames and subjected to optical microscopy.

2.2 Statistical analysis

The results of the geochemical analyses were interpreted using the multivariate statistical analysis. In the study, the following multivariate statistical analyses were used to interpret the data: descriptive statistics, correlation analysis, factor analysis, and cluster analysis. The statistical analyses were conducted using the SPSS 23 software package.

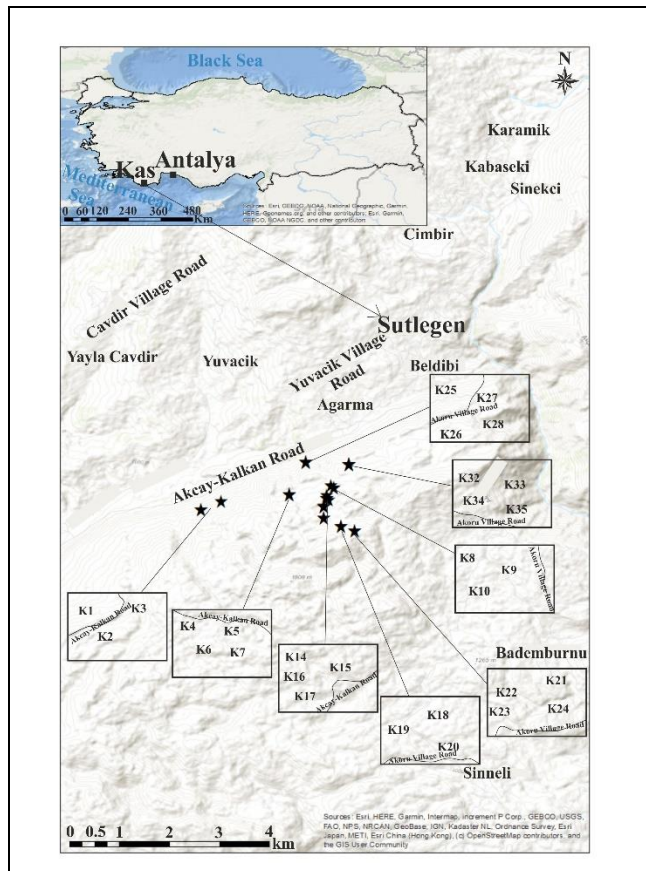


Figure 1. Location map of the study area and samples in Sutlegen.

2.3 Spatial statistics

The geographical coordinates of the locations where the samples were collected in the study area were arranged as latitude (Y) and longitude (X). The coordinates of the sample locations, sample codes, and the results of the geochemical analyses (Table 1) were imported into the ArcMap 10.7

software. The polygons, which include the data laid over the basemap of Turkey, were converted into the raster data format. The distribution map of the geochemical data of SiO₂, MgO, K₂O, Al₂O₃, Fe₂O₃, TiO₂, Mn, Sr, and Co in the region was generated in the raster data format by using the Kriging interpolation method (Figure 2 and Figure 3).

Table 1. Results of the chemical analysis of the limestone samples.

	Latitude	Longitude	CaO (%)	MgO (%)	SiO ₂ (%)	Al ₂ O ₃ (%)	Fe ₂ O ₃ (%)	SO ₃ (ppm)	P ₂ O ₅ (%)	K ₂ O (%)	TiO ₂ (%)	Sr (ppm)	Mn (%)	Sn (ppm)	Cl (ppm)	Zn (%)	Cu (%)	Y (ppm)
K1	36.39277	29.55527	97.9	0.561	0.766	0.436	0.198	231	0.0264	0.0242	0.00914	96.2	0.0177	50.2	0	0.00323	0.00304	52.9
K2	36.39277	29.55527	98	0.542	0.682	0.437	0.12	229	0.026	0.0292	0.0121	71	0.0161	58.7	47.1	0.00271	0.00188	28.4
K3	36.39510	29.56111	96.9	0.465	1.07	1.06	0.279	278	0.0275	0.0307	0.0527	114	0.0176	55.4	66.5	0.00312	0.00223	33.3
K4	36.55913	29.56277	97.9	0.446	0.581	0.35	0.493	373	0.0251	0.032	0.00616	360	0.0116	61.7	52.3	0.00321	0.00134	23
K5	36.55913	29.56277	98.8	0.409	0.281	0.215	0.146	229	0.0255	0.0221	0	103	0.00577	52.2	56.6	0.00288	0.00197	0
K6	36.55913	29.56277	98.7	0.505	0.287	0.201	0.0813	628	0.0426	0.0236	0	232	0.0142	59.4	47.6	0.00374	0.00299	0
K7	36.39695	29.58083	98.9	0.357	0.269	0.217	0.0608	296	0.0208	0.0193	0	282	0.00882	58.3	0	0.0028	0.00228	24.9
K8	36.39945	29.59277	98.7	0.349	0.385	0.276	0.0882	353	0.0237	0.032	0.0047	258	0.00855	59.8	57.8	0.00295	0.00314	0
K9	36.39889	29.59361	98.6	0.307	0.417	0.374	0.136	266	0.0231	0.0268	0.00775	184	0.0177	45	61.8	0.00294	0.00289	0
K10	36.39889	29.59361	99.2	0.249	0.143	0.143	0.0774	193	0.021	0.0134	0	126	0.00531	53.1	0	0.00272	0.0018	39.4
K11	36.39668	29.59166	99.2	0.235	0.161	0.172	0.0864	192	0.0209	0.0209	0	146	0	57.9	52	0.003	0.00254	39.9
K12	36.39589	29.59166	99.3	0.199	0.165	0.183	0.0481	178	0.019	0.0186	0	117	0	61.7	49.3	0.0025	0.0021	35.6
K13	36.39589	29.59166	99.2	0.177	0.146	0.16	0.144	281	0.0212	0.0174	0	80.9	0.0143	65.9	79.3	0.00749	0.00248	15.8
K14	36.39589	29.59166	99.1	0.206	0.2	0.186	0.088	247	0.0221	0.0171	0	88.9	0.0118	53.8	62.6	0.00382	0.00215	38.8
K15	36.39556	29.59222	99.3	0.215	0.154	0.117	0.052	212	0.0187	0.0249	0	101	0.0184	53.5	61.3	0.0031	0.00217	0
K16	36.39381	29.59083	99.4	0.256	0.0912	0.12	0.0277	201	0.0195	0.0156	0	156	0.00918	49.3	53.7	0.00219	0.00156	27.1
K17	36.39361	29.59083	99.3	0.24	0.147	0.146	0.0421	253	0.0243	0.0222	0	145	0.00569	0	46.7	0.00252	0.00225	0
K18	36.39361	29.59083	99.2	0.24	0.165	0.166	0.043	240	0.0209	0.0207	0	158	0	52	43.8	0.00268	0.00177	0
K19	36.39055	29.59083	99.2	0.24	0.138	0.162	0.0886	223	0.0234	0.024	0	150	0.0209	54.4	66.6	0.00315	0.00213	9.06
K20	36.39055	29.59083	99.4	0.241	0.0868	0.124	0.0367	191	0.0198	0.0219	0	148	0.0109	56	0	0.00299	0.00254	0
K21	36.38833	29.59583	99.1	0.209	0.237	0.252	0.0773	221	0.0222	0.0302	0	0	0.00615	54	67.6	0.00295	0.00198	0
K22	36.38833	29.59583	99.3	0.198	0.135	0.16	0.0753	173	0.022	0.0187	0	156	0.011	0	0	0.00284	0.00272	0
K23	36.38695	29.59972	96	0.253	1.5	1.24	0.652	291	0.0637	0.0682	0.0595	123	0.024	60.5	50.6	0.00367	0.00246	29.6
K24	36.38695	29.59972	99.1	0.27	0.171	0.187	0.0925	239	0.0222	0.023	0	138	0.0208	63.8	0	0.00283	0.00112	30.7
K25	36.40583	29.58555	98.2	0.255	0.205	0.231	0.919	291	0.024	0.02	0	136	0.00686	60.7	0	0.0023	0.00195	29.6
K26	36.40583	29.58555	97.8	1.11	0.294	0.235	0.0735	1250	0.016	0.0363	0.00591	663	0.0152	0	65.1	0.00314	0.00021	8.83
K27	36.40583	29.58555	99.91	0.348	0.116	0.135	0.0889	318	0.0218	0.0263	0	0	0.0122	60.8	49.8	0.00273	0.0024	0
K28	36.40583	29.58555	97.4	1.2	0.51	0.324	0.127	1350	0.149	0.0284	0.0081	699	0.0121	67.1	79.6	0.00269	0.00172	28.5
K29	36.40527	29.59805	98.6	0.366	0.17	0.189	0.422	381	0.0221	0.0246	0	338	0.106	51.7	52.2	0.00305	0.0027	28.8
K30	36.40527	29.59805	98.7	0.404	0.287	0.301	0.0643	317	0.0219	0.0242	0	355	0.0191	55.5	54.5	0.00239	0.00201	0
K31	36.40527	29.59805	98.7	0.533	0.202	0.229	0.0581	489	0.0236	0.0268	0.00549	384	0.0125	54.5	70.6	0.00304	0.0233	12
K32	36.40527	29.59805	99.3	0.299	0.0894	0.129	0.0297	236	0.0189	0.0241	0	210	0.0249	59.3	66.8	0.00331	0.00238	0
K33	36.40527	29.59805	98.3	0.562	0.434	0.368	0.0852	521	0.0231	0.0316	0.0123	429	0.00837	64.4	66	0.00287	0.00273	11.5
K34	36.40527	29.59805	99.3	0.248	0.105	0.138	0.0277	219	0.0185	0.0283	0	186	0.00042	50.1	95	0.00251	0.00268	0
K35	36.40527	29.59805	94.5	0.403	0.268	0.288	1.19	460	0.0224	0.0224	0	327	0.136	60.6	95	0.00275	0.00237	51.3

	Cr (%)	Pb (ppm)	Cd (ppm)	Te (ppm)	Th (ppm)	Ta (ppm)	Co (%)	Rb (ppm)	As (%)	U (ppm)	W (ppm)	In (ppm)	Au (ppm)	Tl (ppm)	Ir (ppm)	Pt (ppm)	Hg (ppm)	Se (%)
K1	0.00198	19.1	24.4	0	0	0	0	0	0	0	0	13	0	0	0	0	0	0
K2	0.0036	0	0	0	0	13.9	0	0	0	0	0	0	0	0	0	0	0	0
K3	0.00231	14.7	0	0	0	0	0	0	0	0	0	0	8.2	0	0	0	0	0
K4	0.00203	15.6	0	24	0	0	0	5.33	0.000492	0	0	0	0	0	0	0	0	0
K5	0	0	0	20.8	0	0	0	0	0	0	0	0	0	0	0	0	0	0.000354
K6	0.00295	0	0	0	0	0	0	0	0	0	0	0	0	0	0	0	0	0
K7	0.00286	0	0	27.2	0	0	0	0	0	0	0	0	0	0	0	0	0	0
K8	0.000927	0	0	30.5	0	0	0	0	0	0	0	0	0	0	0	0	0	0
K9	0.00322	0	0	0	0	0	0	0	0	0	0	0	0	0	0	0	0	0
K10	0.00107	0	0	37.8	0	15.5	0	0	0	0	0	0	0	0	0	0	0	0
K11	0.00143	0	30.2	0	0	0	0	0	0	0	0	0	0	0	0	0	0	0
K12	0	0	9.45	0	0	0	0	0	0	0	0	0	0	0	0	0	0	0
K13	0.000926	9.83	63.9	0	0	0	0	0	0.000712	0	0	0	0	0	0	0	0	0
K14	0.00136	11.2	119	0	0	14.2	0	0	0	0	0	0	0	0	0	0	0	0
K15	0	0	20.8	0	0	28.5	0	0	0	0	0	0	0	0	0	0	0	0
K16	0	0	0	0	0	0	0	0	0	0	0	0	0	0	0	0	0	0
K17	0	0	10	17.3	0	0	0	0	0	0	21.9	0	0	0	0	0	0	0
K18	0.000802	99.8	0	0	68.3	17.2	0	0	0	17.9	0	0	0	0	0	0	0	0
K19	0	7.93	0	16.4	0	26.8	0	0	0	0	0	0	0	0	12.9	0	0	0
K20	0	0	0	0	0	0	0.00148	0	0	0	0	0	0	0	0	0	0	0
K21	0.00123	0	0	24.8	0	0	0	0	0	0	0	0	0	0	0	0	0	0
K22	0	0	0	0	0	0	0	0	0	0	0	0	0	0	0	0	0	0
K23	0.00241	15.3	0	0	0	0	0	9.15	0	0	0	0	0	0	0	0	0	0
K24	0	0	9.66	0	0	20.9	0	0	0	0	17.4	0	0	0	0	0	0	0
K25	0	13.8	0	0	0	0	0.00294	0	0.000312	0	0	0	10.1	0	0	0	0	0
K26	0.00433	0	0	26	0	19.9	0	0	0	0	0	0	0	0	0	0	0	0
K27	0.00197	0	0	29.4	0	0	0	0	0	0	0	0	0	0	0	0	0	0
K28	0.00205	9.52	0	0	0	0	0	0	0	0	0	0	0	0	0	0	0	0
K29	0	8.56	0	0	0	0	0.00375	0	0.00111	0	0	0	0	0	0	0	0	0
K30	0.00115	78.8	0	0	54.5	0	0	0	0	11.8	17.4	0	8.23	6.54	0	9.76	0	0
K31	0.00115	0	0	23	0	23.3	0	0	0	0	0	0	0	0	0	0	0	0
K32	0.00151	0	0	0	0	14.1	0	50.7	0	0	0	0	0	0	0	0	0	0
K33	0	0	0	0	0	0	0	0	0	0	0	0	0	0	0	0	0	0
K34	0.0017	111	0	0	76	0	0	0	0	19.2	0	0	12.9	0	0	0	9.18	0
K35	0	10.7	0	0	0	0	0.00739	0	0.00259	0	0	0	0	0	0	0	0	0

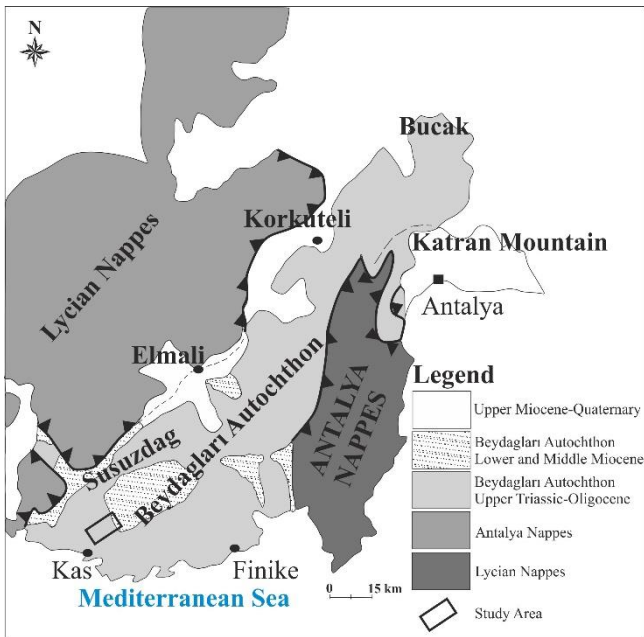


Figure 2. Major tectonic belts of the Western Taurides (modified after [21]).

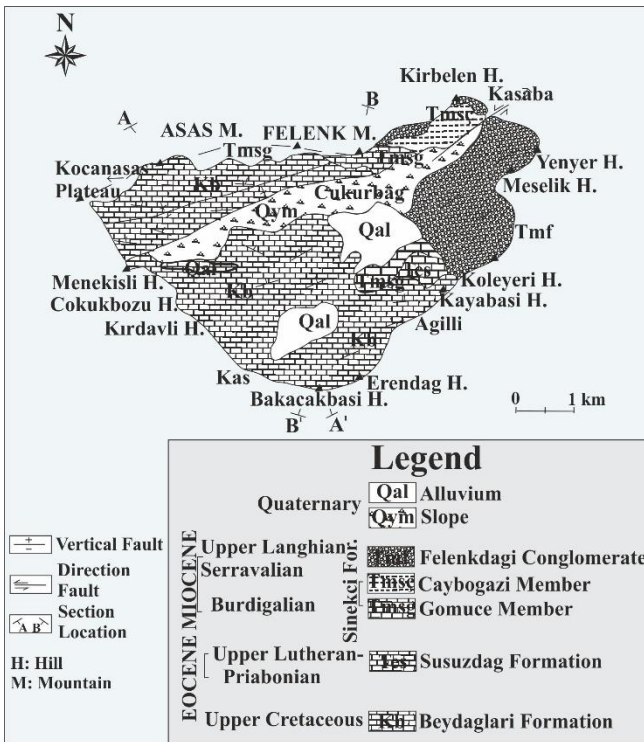


Figure 3. Geological map of the study area (modified after [23]).

2.4 Regional geology

The study area, which lies within the borders of Katran Mountain, is located in the Beydaglari carbonate platform. The Beydaglari carbonate platform is bounded by the Lycian Nappes in the west and Antalya Nappes in the east [16]. The Beydaglari Autochthon had a formation mainly with basin and oceanic crust genesis [17]. The age range of the Beydaglari limestone formation was found to be Jurassic-Cretaceous [18].

Also, it was found that the Beydaglari Autochthon consisted of 2 units, namely the Antalya Union and the Elmali Union. Moreover, these units were observed to contain limestones of various age ranges and chemical properties [19]. In general, the Beydaglari Autochthon is studied under the following 4 (four) formations: Late Cretaceous Beydaglari Formation, Eocene aged Susuzdag Formation, Miocene aged Sinekci Formation, and Kasaba Formation [12]. While Beydaglari Formation and Susuzdag Formation are characterized by neritic limestones, the Sinekci Formation and Kasaba Formation are characterized by various types of sedimentary rocks [12],[20]. With the Upper Miocene allochthonous units that were overlain on the Beydaglari Autochthon, the extension regime prevailed in the region [12]. The tectonic activity that took place in the Pliocene has been going on and increased in the field, thus, developing normal and strike-slip faults in the region. In this context, the region took its present morphological form after the Langhian age [12]. The limestone sequences in the Western Taurides are generally rudist-bearing shallow-water limestones [21],[22].

It was stated that the Kas district of Antalya province was characterized by light gray calcareous formations and showed a bedded structure. The carbonate formations observed in the study area showed inconsistent presence with each other [12], [23], [24]. In the region, the carbonate rocks were collected in two formation and three member: Beydaglari Formation (Kb), Susuzdag Formation (Tes), Gomuce Member (Tmsg), Caybogazi Member (Tmsc), Felenkdagi Conglomerate (Tmf) (Figure 2).

Beydaglari Formation (Kb): The Liassic-Late Cretaceous aged unit, which has spread on a wide area, consists of neritic limestones [23].

Susuzdag Formation (Tes): The unit, which contains the nummulites, consists of the medium-thick bedded limestone and recrystallized limestones. The formation is an Late Lutetian-Priabonian aged unit [23].

Gomuce Member (Tmsg): The formation, which consists of algal limestones, is a Burdigalian aged unit [23].

Caybogazi Member (Tmsc): The formation, which contains various sedimentary formations (sandy limestone, marl, conglomerate, etc.) is a Burdigalian aged unit [23].

Felenkdagi Conglomerate (Tmf): The Upper Langhian-Serravalian aged unit consists of thick-bedded conglomerates [23].

3 Results and discussion

The results of the chemical analysis of the limestone samples collected from Susuzdag Formation, sample codes, and sample location coordinates in terms of latitude and longitude are presented in Table 1.

3.1 Distribution maps

The distributions of some of the major and trace elements obtained from the results of the chemical analysis were generated according to the coordinates of the sample locations in the study area by using the ArcMap 10.7 software (Figure 4 and Figure 5).

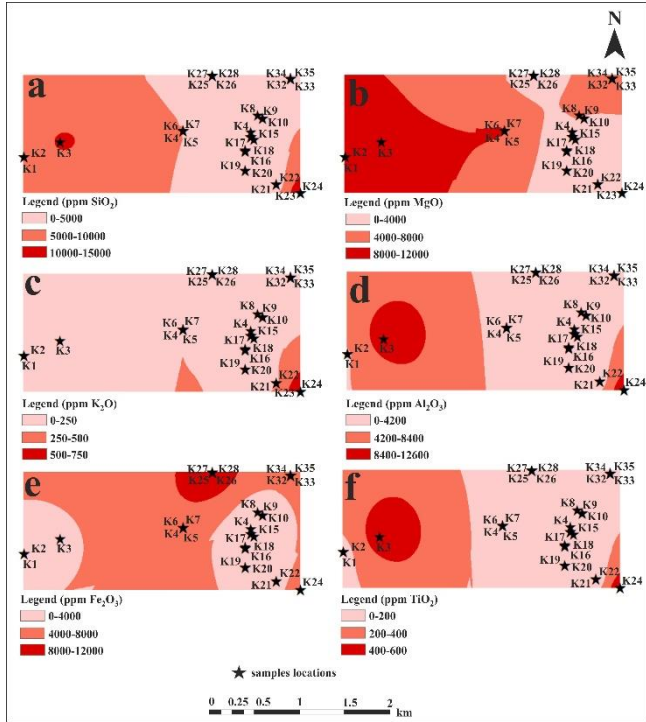


Figure 4. Spatial distribution maps of the major element concentrations of the limestone samples; a)SiO₂ b)MgO c)K₂O d)Al₂O₃ e)Fe₂O₃ f)TiO₂.

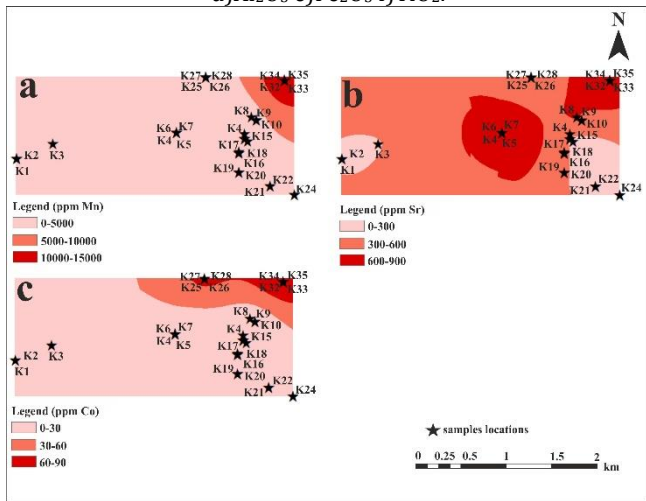


Figure 5. Spatial distribution maps of the trace element concentrations of the limestone samples; a)Mn b)Sr c)Co.

The following results were obtained from the spatial distribution maps generated according to the coordinates of the chemical data:

In the study area, the distribution of SiO₂ was found to increase in direct proportion with the major components of K₂O and TiO₂. Considering the general geology of the region, it is represented by carbonate units. In this context, it is expected that the major oxides of SiO₂ and K₂O, which are rock-forming components, will act in direct proportion in the formation of limestones in the region. The fact that TiO₂ major oxide has a similar relationship with the major rock-forming oxides has been associated with the ultrabasic rocks in the region. The direct proportional increase of the referee's SiO₂-K₂O-TiO₂ has been associated with regional geology.

The distribution of Al₂O₃ was found to increase in direct proportion with the major components of SiO₂ and TiO₂.

The high values of K₂O, Al₂O₃, SiO₂ show the presence of clay minerals in the limestone samples taken from that region (Figure 5-a, c, d).

The high values of Al₂O₃ and TiO₂ elements indicate the presence of minerals rich in aluminum oxides in the limestone samples in that location (Figure 5-d, f).

The trace elements of Co and Mn, which took part in the formation of the limestones, were found to increase in direct proportion.

3.2 Multi-Variable statistical analyses

3.2.1 Descriptive statistics

Table 2 presents the geochemical data obtained from the results of the analyses. The mean values of the major elements concentrations of the limestone samples were calculated and listed in % in descending order as follows: CaO (96.01±2.53) > MgO (0.37±0.038) > SiO₂ (0.31±0.050) > Al₂O₃ (0.27±0.040) > Fe₂O₃ (0.18±0.043) > SO₃ (0.034±0.004) > P₂O₅ (0.027±0.0038) > K₂O (0.025±0.0015) > TiO₂ (0.005±0.0022). The mean values of the trace elements concentrations of the limestone samples were calculated and listed in ppm in descending order as follows: Sr (207.46±26.69) > Mn (180.03±45.32) > Sn (52.04±2.86) > Cl (49.08±4.67) > Zn (30.52±1.45) > Cu (27.99±6.11) > Y (17.11±2.89) > Cr (12.28±2.05) > Pb (12.17±4.59) > Cd (8.21±3.90) > Te (7.92±2.08) > Th (5.68±3.21) > Ta (5.55±1.58) > Co (4.45±2.47) > Rb (1.86±1.47) > As (1.49±0.82) > U (1.40±0.80) > W (1.12±0.79) > In (0.87±0.61) > Au (0.84±0.48) > Tl (0.48±0.34) > Ir (0.37±0.37) > Pt (0.28±0.28) > Hg (0.26±0.26) > Se (0.10±0.10).

Table 2. Descriptive statistics of the limestone samples.

	Mean	Median	Mode	Standard Deviation
CaO	960117.1496.01±25385.292.53	98.80	99.3	15.9
MgO	3742.000.37±383.510.038	0.29	0.24	0.22
SiO ₂	3159.540.31±504.220.050	0.20	0.16	0.29
Al ₂ O ₃	2757.430.27±400.030.040	0.20	0.16	0.23
Fe ₂ O ₃	1805.370.18±437.910.043	0.08	0.02	0.25
SO ₃	344.290.034±44.010.004	0.02	0.02	0.02
P ₂ O ₅	275.110.027±38.270.0038	0.02	0.02	0.02
K ₂ O	254.200.025±15.330.0015	0.02	0.02	0.00
TiO ₂	52.530.005±22.420.0022	0.00	0.00	132.66
Sr	207.46±26.69	150.00	0.00 ^a	157.90
Mn	180.03±45.32	121.00	0.00	268.10
Sn	52.04±2.86	55.50	0.00	16.91
Cl	49.08±4.67	53.70	0.00	27.62
Zn	30.52±1.45	29.40	29.50	20302.00
Cu	27.99±6.11	22.50	25.40	36.14
Y	17.11±2.89	12.00	0.00	44425.00
Cr	12.28±2.05	18568.00	0.00	42339.00
Pb	12.17±4.59	0.00	0.00	27.18
Cd	8.21±3.90	0.00	0.00	44431.00
Te	7.92±2.08	0.00	0.00	12389.00
Th	5.68±3.21	0.00	0.00	44215.00
Ta	5.55±1.58	0.00	0.00	12298.00
Co	4.45±2.47	0.00	0.00	14.61
Rb	1.86±1.47	0.00	0.00	25051.00
As	1.49±0.82	0.00	0.00	31138.00
U	1.40±0.80	0.00	0.00	26755.00
W	1.12±0.79	0.00	0.00	24198.00
In	0.87±0.61	0.00	0.00	22706.00
Au	0.84±0.48	0.00	0.00	31079.00
Tl	0.48±0.34	0.00	0.00	44198.00
Ir	0.37±0.37	0.00	0.00	43132.00
Pt	0.28±0.28	0.00	0.00	23743.00
Hg	0.26±0.26	0.00	0.00	20090.00
Se	0.10±0.10	0.00	0.00	0.60

The box plot used for descriptive statistics is given in Figure 6.

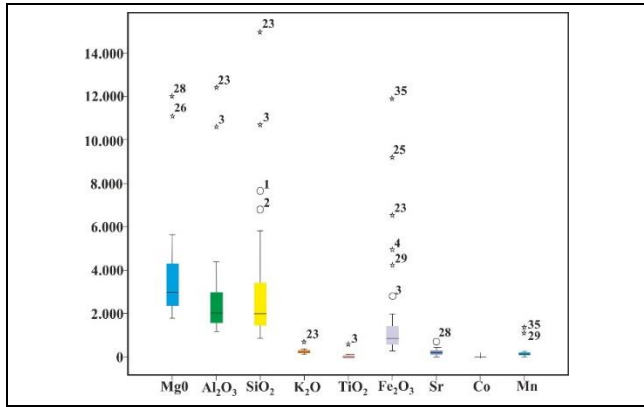


Figure 6. Box plot of the MgO, Al₂O₃, SiO₂, K₂O, TiO₂, Fe₂O₃, Sr, Co, and Mn concentrations of the limestone samples.

The distribution of the MgO concentration was found to range between 2000 ppm and 6000 ppm. Sample 26 and Sample 28 were found to be out of this range. The distribution of Al₂O₃ concentration was found to range between 0 ppm and 4000 ppm, where Sample 3 and Sample 23 were out of this range. The distribution of the SiO₂ concentration was found to range between 0 ppm and 4000 ppm. Sample 1, Sample 2, Sample 3, and Sample 23 were found to be out of this range. The distribution of the K₂O concentration was found to range between 0 ppm and 2000 ppm, where Sample 23 was found to be out of this range. The distribution of the TiO₂ concentration was found to range between 0 ppm and 2000 ppm, where Sample 3 was found to be out of this range. The distribution of the Fe₂O₃ concentration was found to range between 0 ppm and 2000 ppm. Sample 3, Sample 4, Sample 23, Sample 25, Sample 29, Sample, and Sample 35 were found to be out of this range. The distribution of the Sr concentration was found to range between 0 ppm and 2000 ppm, where Sample 28 was found to be out of this range. The distribution of the Co concentration was found to range between 0 ppm and 2000 ppm. No sample was found to be out of this range. The distribution of the Mn concentration was found to range between 0 ppm and 2000 ppm. Sample 29 and Sample 35 were found to be out of this range.

3.2.2 Correlation analysis

According to the central limit theorem, the normality hypothesis is accepted for the data size $n \geq 30$ [8], [25]-[31]. In this context, Pearson's correlation coefficients were used to examine the correlations between the geochemical data of the limestone samples (Table 3).

The elemental correlations were calculated using Pearson's correlation analysis. The elements with very strong positive correlations are as follows: MgO with SO₃ (0.920**); Al₂O₃ with SiO₂ (0.961**) and TiO₂ (0.920**); SO₃ with Sr (0.862**); Mn with Co (0.870**) and As (0.891**); Co with As (0.908**); Pb with Th (0.975**) and U (0.973**); Th with U (0.997**). The elements with strong positive correlations are as follows: MgO with Sr (0.809**); Al₂O₃ with K₂O (0.764**); SiO₂ with K₂O (0.778**); K₂O with TiO₂ (0.761**); Fe₂O₃ with Co (0.802**) and As (0.758**).

3.2.3 Regression analysis

Considering the spatial distribution maps generated for the study area and Pearson's correlation table in which the elemental correlations were revealed, Al₂O₃-SiO₂ and Al₂O₃-TiO₂ associations were found to play a key role in the formation of limestones in the region. The statistical explanation of these correlations was tested using the simple regression analysis. The scatter diagrams generated using the results of the regression analysis and the R² (explained variance) values are given in Figure 7-a, b.

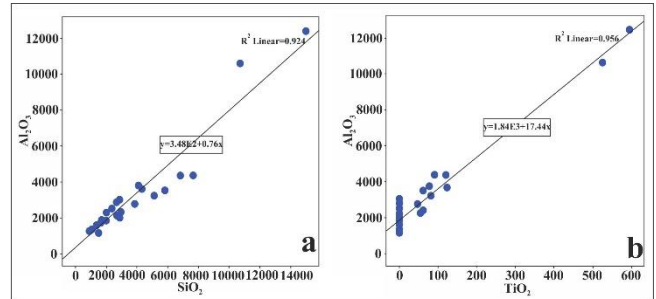


Figure 7. Scatter diagrams a) Al₂O₃-SiO₂ b) Al₂O₃-TiO₂.

Table 3. Pearson's correlation coefficients calculated using the results of the chemical analysis of limestone samples.

	MgO	AlO ₃	SiO ₂	P ₂ O ₅	SO ₃	Cl	K ₂ O	CaO	TiO ₂	Fe ₂ O ₃	Cr	Mn	Co	Cu	Zn	As	Se	Rb	Sr	Y	Cd	In	Su	Te	Ta	W	Pr	Ir	Au	Tl	Hg	Pb	Th	U	
MgO	1																																		
Al ₂ O ₃	0.158	1																																	
SiO ₂	0.269	0.961**	1																																
P ₂ O ₅	0.589**	0.293	0.371*	1																															
SO ₃	0.920**	0.05	0.12	0.634**	1																														
Cl	0.219	0.093	0.046	0.172	0.308	1																													
K ₂ O	0.253	0.764**	0.778**	0.314	0.249	0.246	1																												
CaO	-0.008	0.058	0.071	0.02	-0.008	-0.023	-0.054	1																											
TiO ₂	0.15	0.978**	0.920**	0.284	0.059	0.109	0.761**	0.029	1																										
Fe ₂ O ₃	-0.004	0.469*	0.333	0.084	0.048	0.058	0.259	0.007	0.264	1																									
Cr	0.512**	0.372*	0.456**	0.203	0.416*	0.119	0.399*	-0.124	0.349*	-0.113	1																								
Mn	0.057	0.068	0.028	-0.023	0.103	0.245	0.042	-0.004	0.001	0.653**	-0.176	1																							
Co	-0.032	-0.05	-0.106	-0.071	0.047	0.098	-0.103	0.013	-0.124	0.802**	-0.316	0.707**	1																						
Cu	0.061	-0.02	-0.053	-0.037	0.034	0.136	0.025	0.021	0.013	-0.079	-0.034	-0.015*	-0.036	1																					
Zn	-0.107	0.066	0.071	-0.011	0.066	0.215	0.031	0.067	0.085	-0.019	0.112	-0.016	-0.107	0.024	1																				
As	-0.021	-0.032	-0.063	-0.07	0.068	0.286	-0.086	0.011	-0.111	0.758**	-0.237	0.891**	0.908**	-0.041	0.157	1																			
Se	0.027	-0.045	-0.02	-0.015	-0.077	0.047	-0.064	0.032	-0.069	-0.023	-0.176	-0.079	-0.053	-0.04	-0.035	-0.053	1																		
Rb	-0.068	0.025	0.009	-0.018	-0.076	0.114	0.134	0.04	0.06	-0.022	0.082	0.047	-0.067	-0.03	0.078	-0.05	-0.037	1																	
Sr	0.809**	-0.014	0.041	0.466**	0.862**	0.272	0.182	0.206	-0.018	0.076	0.245	0.206	0.137	0.14	-0.133	0.16	-0.115	0.004	1																
Y	0.1	0.393	0.329	0.147	0.099	-0.171	-0.054	0.141	0.237	0.477**	0.021	0.342*	0.363*	0.068	0.008	0.381*	-0.174	-0.143	0.01	1															
Cd	-0.222	-0.127	-0.112	-0.091	-0.143	0.101	-0.253	0.074	-0.124	-0.108	-0.042	-0.085	-0.111	-0.05	0.546**	0.007	-0.062	-0.079	-0.251	0.286	1														
In	0.022	0.019	0.091	-0.038	-0.103	-0.439**	-0.052	0.042	-0.025	-0.041	-0.077	0.014	-0.075	-0.059	-0.015	-0.076	-0.042	-0.053	-0.137	0.334*	0.083	1													
Su	-0.109	0.147	0.158	0.203	-0.137	0.136	0.04	-0.1	0.1	0.198	-0.062	0.086	0.111	0.057	0.162	0.14	0.002	0.1	-0.133	0.293	0.071	0.087	1												
Te	0.104	-0.172	-0.136	-0.154	0.101	-0.091	0.013	-0.294	-0.159	-0.165	0.162	-0.201	-0.201	0.17	-0.111	-0.145	0.182	-0.107	0.07	-0.192	-0.217	-0.159	-0.165	1											
Ta	0.037	-0.218	-0.217	-0.171	0.043	0.02	-0.072	0.118	-0.144	-0.258	-0.012	-0.066	-0.186	0.257	-0.003	-0.188	-0.104	0.128	0.03	-0.079	0.121	0.17	-0.073	0.138	1										
W	-0.067	-0.064	-0.089	-0.047	-0.06	0.01	-0.064	0.05	-0.098	-0.123	-0.147	-0.059	-0.075	0.045	-0.171	-0.076	-0.042	0.053	0.048	-0.249	-0.028	-0.06	-0.405*	0.035	-0.148	1									
Pr	0.023	0.019	-0.017	-0.043	-0.018	0.034	-0.023	0.031	-0.069	-0.078	-0.011	0.007	-0.053	-0.038	-0.135	-0.053	-0.029	-0.037	0.163	-0.174	-0.062	-0.042	0.056	-0.112	-0.104	0.608**	1								
Ir	-0.103	-0.084	-0.104	-0.032	-0.081	0.11	-0.027	0.037	-0.069	-0.062	-0.176	0.019	-0.053	-0.032	0.02	-0.053	-0.029	-0.037	-0.063	-0.082	-0.062	-0.042	0.024	0.12	0.396*	-0.042	-0.029	1							
Au	-0.029	0.212	0.111	-0.074	-0.094	0.291	0.08	0.049	0.216	-0.084	0.122	-0.085	-0.092	-0.036	-0.143	-0.093	-0.051	-0.065	0.011	-0.138	-0.108	-0.073	0.019	-0.194	-0.18	0.244	0.451**	0.051	1						
Tl	-0.065	-0.018	-0.064	-0.044	-0.04	-0.244	-0.101	0.039	-0.097	0.379*	-0.156	-0.058	0.224	-0.056	-0.204	0.02	-0.041	-0.052	0.023	0.012	-0.087	-0.059	0.095	-0.157	-0.145	0.299	0.526**	0.041	0.205	1					
Hg	-0.097	-0.101	-0.123	-0.069	-0.084	0.289	0.055	0.038	-0.069	-0.103	0.068	-0.114	-0.053	0.006	-0.11	-0.053	0.029	0.037	-0.024	-0.174	-0.062	-0.042	-0.02	-0.112	-0.104	0.042	-0.029	0.039	0.736**	0.041	1				
Pb	-0.092	0.011	-0.017	-0.056	-0.092	0.2	0.035	0.08	-0.017	-0.023	0.018	-0.079	-0.028	-0.076	-0.123	-0.016	-0.078	-0.071	0.034	-0.18	-0.05	-0.036	0.056	0.252	-0.032	0.207	0.427*	0.027	0.699**	0.244	0.633**	1			
Th	-0.117	-0.108	-0.145	-0.099	-0.108	0.192	-0.029	0.063	-0.122	-0.163	0.005	-0.145	-0.094	-0.052	-0.186	-0.094	-0.052	-0.066	0.03	-0.308	-0.109	-0.074	0.004	-0.198	0.012	0.241	0.447**	0.052	0.685**	0.202	0.644**	0.975**	1		
U	-0.123	-0.113	-0.148	-0.098	-0.11	0.192	-0.03	0.063	-0.12	-0.163	0.003	-0.15	-0.093	-0.052	-0.181	-0.093	-0.051	-0.065	0.017	-0.305	-0.108	-0.073	0.001	-0.195	0.024	0.201	0.383*	0.051	0.662**	0.167	0.655**	0.973**	0.997**	1	

** Correlation is significant at the 0.01 level (2-tailed). * Correlation is significant at the 0.05 level (2-tailed).

The Al_2O_3 - SiO_2 and Al_2O_3 - TiO_2 associations, which were observed to have a linear positive correlation, are named Model 1 and Model 2 to test the mathematical formation model of the limestones in the region. The explained variance analysis performed for Model 1 and Model 2 and the statistical error of the mathematical model established are given in Table 4 and Table 5, respectively. The estimated coefficients of the mathematical models established are given in Table 6.

Table 4. Coefficient of Determination (Explained Variance).

Model Summary ^b				
Model	R	R Square	Adjusted R Square	Std. Error of the Estimate
1	0.96 ^a	0.92	0.92	662.74
2	0.97 ^a	0.95	0.95	504.39

a. Predictors: (Constant)0. SiO_2 (Model 1); TiO_2 (Model 2)
 b. Dependent Variable: Al_2O_3

Table 5. Statistical Error (Analysis of Variance) Table.

ANOVA ^a						
Model	Sum of Squares	df	Mean Square	F	P-value	
1	Regression	175936842.11	1	175936842.11	400.56	0^b
	Residual	14494426.45	33	439225.04		
	Total	190431268.57	34			
2	Regression	182035518.90	1	182035518.90	715.50	0^b
	Residual	8395749.66	33	254416.65		
	Total	190431268.57	34			

a. Predictors: (Constant)0. SiO_2 (Model 1); TiO_2 (Model 2)
 b. Dependent Variable: Al_2O_3

Table 6. Table of the Coefficients of the Mathematical Model.

Model		Coefficients ^a								
		Unstandardized Coefficients		Standardized Coefficients		t	P-value	Correlations		
B	Std. Error	Beta		Zero-order	Partial			Part		
1	(Constant) (b ₀)	348.04	164.44			2.11	.04			
	SiO_2 (b ₁)	0.76	0.03	0.96	20.01	0	0.96	0.96	0.96	
2	(Constant) (b ₀)	1841.24	91.88			20.03	0			
	TiO_2 (b ₁)	17.44	0.65	0.97	26.74	0	0.97	0.97	0.97	

a. Predictors: (Constant)0. SiO_2 (Model 1); TiO_2 (Model 2)
 b. Dependent Variable: Al_2O_3

In the Coefficient of Determination table, the R^2 values were calculated for both models established. The R^2 value for the Al_2O_3 - SiO_2 model was found to be 0.92, while the R^2 value for the Al_2O_3 - TiO_2 model was calculated as 0.95. The explained variance values of the suggested models were found to be high and suitable. In the ANOVA analysis, the probability value (P-value) was calculated as 0 for both mathematical models. Accordingly, these two associations, which played a major role in the formation of limestones, were found to be statistically significant. The probability values (P-values) of the parameter estimates (values of the Beta constants) for the established mathematical models were found to be below 0.05, and they were found to be statistically significant [32]. The fact that the constant values (b₀) have a positive value indicated that they had a linear relationship with the dependent variable [7],[32]-[36]. The mathematical models established for the formation of limestones can be explained at the significance level of 0.05 [32].

3.2.4 Factor analysis

Factor analysis is used to determine the variances of data with similar characteristics and to understand their relationships at the stage of the classification of the geochemical data [8],[37]-[40]. Before conducting the factor analysis, the sampling adequacy of the data for the factor analysis was tested using the Kaiser-Meyer-Olkin test, and the test statistics revealed that the data is suitable [41]-[44] (Table 7).

Table 7. Kaiser-Meyer-Olkin (KMO) Measure of Sampling Adequacy of the geochemical data.

KMO and Bartlett's Test		
Kaiser-Meyer-Olkin Measure of Sampling Adequacy.		0.52
Bartlett's Test of Sphericity	Approx. Chi-Square	731.02
	df	78
	P-value	0

The measure of sampling adequacy is expected to be greater than 0.5 for the suitability of the data for the factor analysis [35], [45]-[50]. In this context, the value that was calculated as 0.52 revealed the suitability of geochemical data for the factor analysis. While the scree plot (Figure 8) reveals the number of factors explaining the geochemical data, Table 8 presents the variances of these factors.

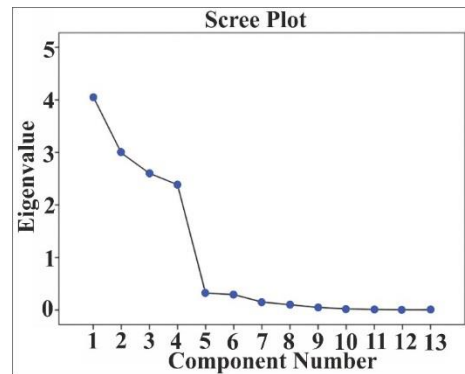


Figure 8. Scree plot of the geochemical data.

The scree plot showed that the slope of the plot began to disappear at Point 4. The scree plot shows that the Eigenvalues of 4 factors are greater than 1. Factor 1 explains 31.24% of the total variance, while Factor 2, Factor 3, and Factor 4 cumulatively explain 54.24%, 74.25%, and 92.60% of the total variance, respectively (Table 8).

Table 8. Total Variance Explained according to Factor Analysis.

Component	Total Variance Explained					
	Initial Eigenvalues			Extraction Sums of Squared Loadings		
	Total	% of Variance	Cumulative %	Total	% of Variance	Cumulative %
1	4.06	31.24	31.24	4.06	31.24	31.24
2	2.99	22.99	54.24	2.99	22.99	54.24
3	2.60	20.01	74.25	2.60	20.01	74.25
4	2.38	18.35	92.60	2.38	18.35	92.60
5	0.32	2.48	95.09			
6	0.29	2.26	97.35			
7	0.15	1.19	98.54			
8	0.10	0.76	99.31			
9	0.04	0.37	99.69			
10	0.02	0.15	99.85			
11	0.01	0.08	99.93			
12	0.008	0.05	99.99			
13	0.001	0.009	100			

The number of factors extracted for the geochemical data and the cumulative variances explained for these factors were calculated. The principal component analysis was applied to reveal the geochemical compositions of the factors statistically (Table 9) [29], [51]-[54]. The geochemical components explaining each factor were revealed. The geochemical components explaining Factor 1 were found to be SiO_2 , Al_2O_3 ,

K₂O, and TiO₂, and the total variance explained by these components was found to be 31.24%. The geochemical components explaining Factor 2 were found to be Pb, Th, and U, and the total variance explained by these components was found to be 22.99%. The geochemical components explaining Factor 3 were found to be MgO, SO₃, and Sr, and the total variance explained by these components was found to be 20.01%. The geochemical components explaining Factor 4 were found to be Fe₂O₃, Mn, and Co, and the total variance explained by these components was found to be 18.35%. The principal component matrix and plot of these factors and their components are shown in Table 9 and Figure 9, respectively.

Table 9. Principal components matrix of the geochemical data.

Component Matrix ^a				
	Components			
	1	2	3	4
SiO ₂	0.86	0.38	-0.21	-0.01
Al ₂ O ₃	0.85	0.40	-0.27	0.06
K ₂ O	0.77	0.40	-0.04	-0.03
MgO	0.48	-0.08	0.73	-0.38
SO ₃	0.42	-0.15	0.80	-0.32
TiO ₂	0.82	0.41	-0.29	-0.01
Fe ₂ O ₃	0.49	-0.20	0.03	0.75
Pb	-0.30	0.81	0.33	0.35
Mn	0.27	-0.40	0.23	0.74
Sr	0.32	-0.11	0.86	-0.17
Co	0.14	-0.43	0.23	0.84
Th	-0.41	0.79	0.34	0.27
U	-0.42	0.79	0.34	0.27
Initial of Variance (%)	31.24	22.99	20.01	18.35

Extraction Method: Principal Component Analysis, a. 4 components were extracted.

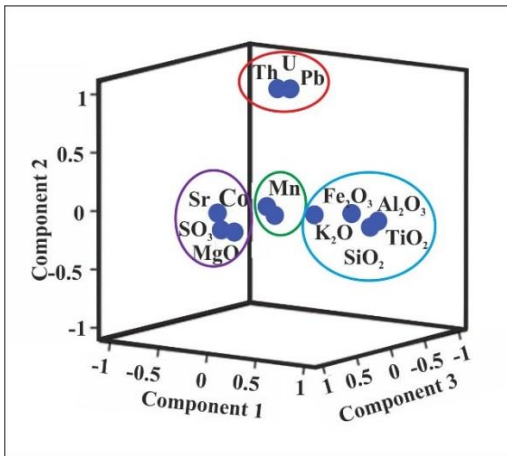


Figure 9. Principal components plot of the geochemical data.

3.2.5 Cluster analysis

The hierarchical classification of the geochemical data of the limestone samples is shown in Figure 10.

Hydrothermal fluids may differentiate the contents of the dominant rocks in the region [55]. Hierarchically, the geochemical data, except for CaO, were observed to be similar, which could be interpreted that CaO had a similar relationship with other geochemical data from a distance. In this context, the difference between CaO and other geochemical major and trace elements indicated the presence of ultrabasic liquids dominant in the region.

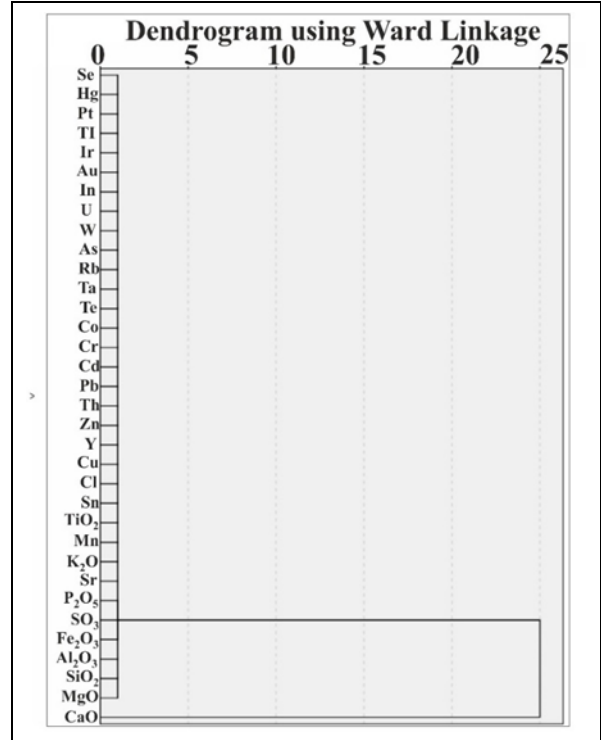


Figure 10. Hierarchical clustering of the geochemical data.

3.3 Mineralogical Features

The thin cross-section microscope images of 5 limestone samples collected from the Susuzdag Formation are given in Figure 11-a, b, c, d, e, and f.

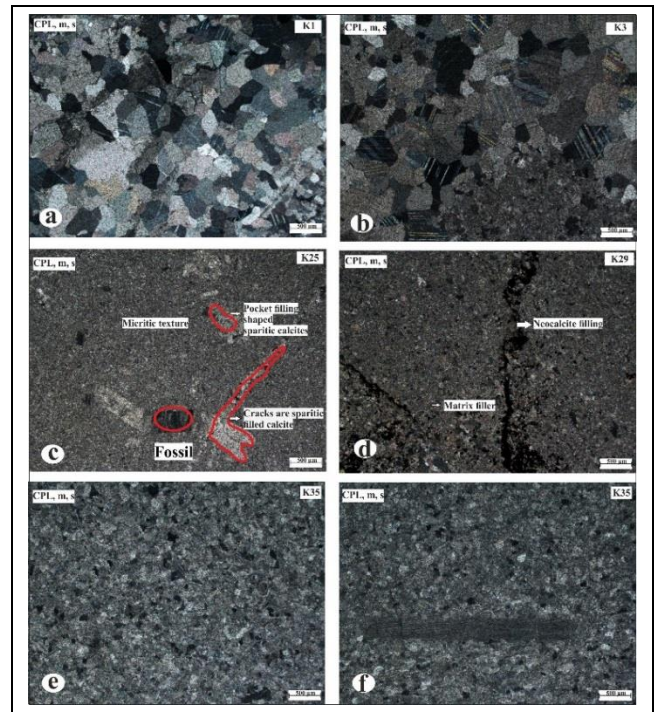


Figure 11. Thin cross-section microscope images (CPL: crossed-polarized light; m: matrix; s: stratification).

According to the results of the examination of the cross-sections under the microscope, the following findings were obtained:

- The cross-sections were found to show very similar mineralogical properties with each other (Figure 11-a, b, c, d, e, f),
- The cross-sections showed micritic and sparitic texture features (Figure 11-a, b, c, d, e, f),
- Limestone samples showed a recrystallized feature. They were observed to have coarse and medium crystalline with equal grain size (Figure 11-a, b, c, d, e, f),
- No porosity was observed in the cross-sections, which confirmed that the limestones had a massive form (Figure 11-a, b, c, d, e, f),
- The cross-sections were observed to contain a small content of fossil (organic sediments) (Figure 11-c),
- Physical properties such as foliation and lamination were not observed in the cross-sections (Figure 11-a, b, c, d, e, f),
- The single-nicol images of the limestone samples showed that the matrix filling was rich in clay content (Figure 11-d),
- The clay content in the matrix filling was thought to be micrite (Figure 11-e),
- The grain sizes of calcite mineral in the (Figures 11 -a, b) are similar each other and similar each other in the (Figures 11-c, d, e, f).

3.4 Paleoenvironmental characteristics of the limestone samples

The Al₂O₃-SiO₂-Fe₂O₃ ternary diagram of the limestone samples was drawn according to [55]-[57] to understand the geochemical formation mechanisms of the limestones, (Figure 12) [55]-[57].

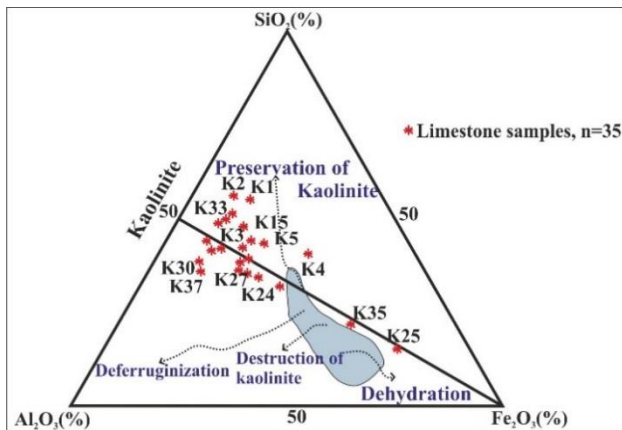


Figure 12. Geochemical ways of formation mechanism (after [55]-[57]).

According to the diagram, the limestones were formed by the enrichment of kaolinite as a result of the decrease in dehydration reactions in the environment. The clay mineral observed in matrix fillings of the thin cross-sections were thought to be kaolinite.

The Chemical Index of Alteration (CIA), which is one of the chemical weathering indices, provides information about the physical and chemical environmental conditions and paleo-redox states of the rock [58]-[59]. The CIA value is calculated using the major elements that constitute the rock by use of the following equation:

$$CIA = \left[\frac{Al_2O_3}{(Al_2O_3 + Na_2O + K_2O + CaO^*)} \right] \times 100 \quad [20] \quad (1)$$

$$CaO^* = ml\ CaO - \left[\left(\frac{10}{3} \right) \times mol\ P_2O_5 \right] \quad (2)$$

The values of the Chemical Index of Alteration calculated for the limestone samples are given in Table 10.

Table 10. CIA values of the limestone samples.

	CIA
K1	0.44
K2	0.44
K3	1.08
K4	0.36
K5	0.22
K6	0.20
K7	0.22
K8	0.28
K9	0.38
K10	0.14
K11	0.17
K12	0.18
K13	0.16
K14	0.19
K15	0.12
K16	0.12
K17	0.15
K18	0.17
K19	0.16
K20	0.12
K21	0.25
K22	0.16
K23	1.28
K24	0.19
K25	0.23
K26	0.24
K27	1.35
K28	0.33
K29	0.19
K30	0.30
K31	0.23
K32	0.13
K33	0.37
K34	0.14
K35	0.30

The CIA values calculated for the limestone samples collected from the Seydisehir district of the Konya province were found to range between 0 and 10 [10]. On the other hand, the CIA values of the limestone samples collected from the Sutlegen village in the Kas district of the Antalya province were found to range between 0 and 1.35.

4 Conclusion

In the present study, the major and trace element concentrations of 35 limestone samples collected to represent the Susuzdag Formation were analyzed. According to the results of the analyses, the major oxides constituting the limestones were found to be CaO, MgO, SiO₂, Fe₂O₃, Al₂O₃, SO₃, P₂O₅, K₂O, and TiO₂ while the trace elements constituting the limestones were found to be Sr, Mn, Sn, Cl, Zn, Cu, Y, Cr, Pb, Cd, Te, Th, Ta, Co, Rb, As, U, W, In, Au, Tl, Ir, Pt, Hg, and Se.

The high values of K_2O , Al_2O_3 and SiO_2 elements of the limestones with the distribution maps indicate the presence of clay minerals; In the regions where Al_2O_3 and TiO_2 elements have high values, the presence of minerals with aluminum oxide and titanium oxide has been considered.

Correlation analysis was performed for the data, which provided the assumption of normality according to the central limit theorem, by calculating Pearson's correlation coefficient. The results of the correlation analysis revealed that CaO, which was one of the major elements constituting the limestone samples, did not correlate with other elements (major and trace elements). The elements with a positive correlation indicated that these components were present in the formation of the limestones and they were enriched in the environment.

Correlation analysis was performed using Pearson's correlation coefficient for the data providing the assumption of normality according to the central limit theorem. According to the results obtained in this context, it was understood that CaO, which was one of the major elements forming limestones, did not establish a correlation with other elements (major and trace). The correlation relations of other major and trace elements provided information about the physical and chemical environmental conditions in which the limestone was formed. Elements in a positive correlation provided information about the components that were present during the formation of limestones and enriched in the environment. The correlations between Al_2O_3 and SiO_2 and between Al_2O_3 and TiO_2 , which were found to be the components with the highest positive correlations, were also tested by regression analysis, and their contribution to the explained variance was discussed statistically. The explained variance (R^2) of the Al_2O_3 and SiO_2 association was found to be 0.92 while the explained variance (R^2) of the Al_2O_3 and TiO_2 association was found to be 0.95. The statistical errors were found to be 0. In this context, it was proved that the massive limestones forming the Susuzdag Formation were among the major components enriched in the environment. The formation of the limestones was explained by 4 factors using the principal component matrix analysis. The components constituting Factor 1 were found to be SiO_2 , Al_2O_3 , K_2O , and TiO_2 , and the total variance explained by this factor was found to be 31.24%. The components constituting Factor 2 were found to be Pb, Th, and U, and the total variance explained by this factor was found to be 22.99%. The components constituting Factor 3 were found to be MgO, SO_3 , and Sr, and the total variance explained by this factor was found to be 20.01%. The components constituting Factor 4 were found to be Fe_2O_3 , Mn, and Co, and the total variance explained by this factor was found to be 18.35%. The contents grouped under the same factors were also found to have strong positive correlations with each other in the correlation analysis.

The hierarchical clustering analysis proved that the major component of CaO did not correlate similarly with other components. The differentiation between CaO and other components revealed the existence of ultrabasic rocks in the region.

The results of the mineralogical examinations of the limestone samples under the optical microscope revealed that the samples reflected the characteristics of the Susuzdag Formation. The thin cross-sections of the samples showed the same physical properties of the formation, which had low porosity and massive structure. The thin cross-sections, which showed sparitic and micritic texture, were observed not to have

foliation and lamination. Moreover, the limestones were found to have a recrystallized form.

The Al_2O_3 - SiO_2 - Fe_2O_3 ternary diagram was generated and the CIA values were calculated to understand the physical and chemical properties of the environment of the limestones and the paleo-redox reactions. According to the results, it was thought that limestones were formed as a result of enrichment in kaolinite minerals by undergoing dehydration reactions in the environment.

5 Author contribution statements

Author 1 and Author 2 ideas, geo-statistical and geo-evaluation of the results obtained in the literature, compilation of analysis samples from the field, laboratory examinations and evaluations of the results, examination and content of the controlled results of the subjects were reviewed.

6 Ethics committee approval and conflict of interest statement

"There is no need to obtain permission from the ethics committee for the article prepared". "There is no conflict of interest with any person/institution in the article prepared".

7 References

- [1] Ekmekçi M, Nazik L. "Evolution of Golpazari-Huyuk karst system (Bilecik-Turkey): indications of morpho-tectonic controls". *International Journal of Speleology*, 33(1), 47-64, 2004.
- [2] Poyraz M, Öztürk MZ, Soykan A. "Sivas Jips Karstında Dolin Yoğunluğunun Cbs Tabanlı Analizi Gis Based Analysis of Doline Density in Sivas Gypsum Karst (Turkey)". *Jeomorfolojik Araştırmalar Dergisi*, 6, 67-80, 2004.
- [3] Abedini A, Calagari AA. "Rare earth element geochemistry of the Upper Permian limestone: the Kanigorgeh mining district, NW Iran". *Turkish Journal of Earth Sciences*, 24(4), 365-382, 2015.
- [4] Ozer O, Yalcin F, Tarinc OK, Yalcin MG. "Investigation of suitability of marbles to standards with inequality expressions and statistical approach using some physical and mechanical properties". *Journal of Inequalities and Applications*, 97, 1-15, 2020.
- [5] Steinmann JW, Grammer GM, Brunner B, Jones CK, Riedinger N. "Assessing the application of trace metals as paleoproxies and a chemostratigraphic tool in carbonate systems: A case study from the "Mississippian Limestone" of the midcontinent, United States". *Marine and Petroleum Geology*, 112, 1-14, 2020.
- [6] Abedini A, Azizi MR, Calagari AA. "Lanthanide tetrad effect in limestone: a tool to environment analysis of the Ruteh Formation, NW Iran". *Acta Geodynamica et Geomaterialia*, 15(3), 229-247, 2018.
- [7] Anfimov AL. "New Emsian foraminifers from of the Karpinsky Horizon limestones Severouralsk Bauxite Mine". *Paleontological Journal*, 46(5), 445-452, 2012.
- [8] Anfimov AL, Soroka EI. "Lithofacies features of boehmite-bearing limestones of the supraore sequence in the north Ural bauxite mine". *Lithology and Mineral Resources*, 50(3), 203-210, 2015.
- [9] Laskou M, Economou-Eliopoulos M. "Bio-mineralization and potential biogeochemical processes in bauxite deposits: genetic and ore quality significance". *Mineralogy and Petrology*, 107(4), 471-486, 2013.

- [10] Temur S, Orhan H, Deli A. "Geochemistry of the limestone of Mortas Formation and related terra rossa, Seydisehir, Konya, Turkey". *Geochemistry International*, 47(1), 67-93, 2009.
- [11] Ozer O. Sutlegen Bölgesi (Kaş, Antalya) Boksit Yataklarının Jenezi ve Ekonomik Özellikleri. Yüksek Lisans Tezi, Akdeniz Üniversitesi, Antalya Türkiye, 2020.
- [12] Şenel M. "Fethiye-M-8 Paftası 1:100.000 Ölçekli Türkiye Jeoloji Haritaları". Maden Tetkik Arama Jeoloji Etütleri Dairesi, Ankara Türkiye, 4, 1997.
- [13] Yalcin F, Kilic S, Nyamsari DG, Yalcin MG, Kilic M. "Principal component analysis of integrated metal concentrations of bogacayı riverbank sediments in Turkey". *Polish Journal of Environmental Studies*, 25(2), 471-485, 2016a.
- [14] Yalcin F, Nyamsari DG, Paksu E, Yalcin MG. "Statistical assessment of heavy metal distribution and contamination of beach sands of Antalya-Turkey: an approach to the multivariate analysis techniques". *Filomat*, 30(4), 945-952, 2016b.
- [15] Oz C, Ozer O. "Seramik Arkeometrisi'nde Spektroskopik Yöntemlerin Uygulanması ve Yorumlanması: XRF, XRD". *Seramik Araştırmaları Dergisi*, 1, 136-153, 2019.
- [16] Poisson A, Poignant AF. "Korkuteli bölgesindeki Miyosen transgresyonunun tabanı olan karabayır formasyonu (Antalya ili)". *Maden Tetkik Araştırma Dergisi*, 82, 65-69, 1977.
- [17] Şenel M. "Batı Toroslar'daki Yeşilbarak Napının stratigrafik ve yapısal özellikleri, GD Anadolu'daki ve Kuzey Kıbrıs'taki benzer birimlerle karşılaştırılması". *Maden Tetkik Araştırma Dergisi*, 128, 1-26, 2004.
- [18] Gültekin MC. "Batı Toroslar Bey Dağları otokton birliğindeki Bey Dağı Formasyonunun Senomaniyen yaşlı karbonat dizilimlerinin mikrofasiyesleri, çökeltme ortamları, karbonat çökeltme modeli ve diyajenezi". Türkiye Petrolleri Anonim Ortaklığı Raporu, Ankara Türkiye, 930, 1986.
- [19] Üşenmez Ş. "Beydağları (Batı Toroslar) otokton kütlesindeki Tersiyer yaşlı karbonat istifi ve bu istifin sedimentolojisi üzerine yapılan çalışmaların ön sonuçları". *Gazi Üniversitesi Mühendislik-Mimarlık Dergisi*, 2, 103-141, 1987.
- [20] Erol A. Finike Yöresi (Batı Toroslar) Limra Mermerlerinin Jeolojisi ve Ekonomik Potansiyeli. Yüksek Lisans Tezi, Dokuz Eylül Üniversitesi, İzmir Türkiye, 2008.
- [21] Sarı B. "Bey Dağları Karbonat Platformu'nun doğu bölümünde orta-üst Senomaniyen platform kireçtaşlarında Geç Kretase yaşlı ardışık pelajik neptüniyen dayk dolguları (Katran Dağ, Antalya, GB Türkiye)". *Yerbilimleri*, 40(1), 35-71, 2019.
- [22] Sarı B, Özer S. "Upper Cretaceous rudist biostratigraphy of the Bey Dağları carbonate platform, western Taurides, SW Turkey". *Geobios*, 42(3), 359-380, 2009.
- [23] Colin HJ. "Fethiye-Kaş-Antalya-Finike (Güneybatı Anadolu) bölgesinde yapılan jeolojik etüdlar". *Maden Tetkik Araştırma Dergisi*, 59, 19-59, 1962.
- [24] Keser N. "Çukurbağ Polyesi'nin jeomorfolojik evrimi". *Marmara Coğrafya Dergisi*, 18, 114-133, 2008.
- [25] Şenel M, Öztürk EM, Özdemir T, Kadıncık G, Metin Y, Serdaroğlu M, Örcen S "Fethiye (Muğla), Kalkan (Antalya) ve Kuzeyinin Jeolojisi". Maden Tetkik Araştırma Raporu, Ankara, Türkiye, 1994.
- [26] Ozer O, Yalcin F, Nyamsari DG, Yalcin MG. "Appraisal of metal accumulation in beach sand using contamination indices and multivariate statistical analysis". *The 2nd Mediterranean International Conference of Pure Applied Mathematics and Related Areas*, Paris, France, 28-31 August 2019.
- [27] Tarinc OK, Ozer O, Aydin B, Yalcin MG. "Comparison of physical-mechanical properties of Clova and Lyca marbles in Akçay (Antalya) region by using independent-samples T-test statistics". *The 2nd Mediterranean International Conference of Pure Applied Mathematics and Related Areas*, Paris, France, 28-31 August 2019.
- [28] Tat E, Yalcin MG. "Rare earth element contents, geochemistry of soil samples between Burdur and Isparta region and assessment of their origin". *Bulletin of the Mineral Research and Exploration*, 162(162), 93-102, 2020.
- [29] Yalcin F, Ozer O, Nyamsari DG, Yalcin MG. "Statistical evaluation of the geochemical content of beach sand along the Sarisu-Kemer coastline of Antalya, Turkey". *American Institute of Physics Conference Proceedings*, 2116, 100005-100009, 2019a.
- [30] Yalcin MG, Unal B. "Multivariate statistical approach to identify heavy metal sources in urban roadside soils of Manisa, Turkey". *Asian Journal of Chemistry*, 20(5), 3978-3990, 2008.
- [31] Yalcin MG, Aydin O, Elhatip H. "Heavy metal contents and the water quality of Karasu Creek in Nigde, Turkey". *Environmental Monitoring and Assessment*, 137(1-3), 169, 2008(b).
- [32] Yalcin MG, Nyamsari DG, Ozer Atakoglu O, Yalcin F. "Chemical and statistical characterization of beach sand sediments: implication for natural and anthropogenic origin and paleo-environment". *International Journal of Environmental Science and Technology*, 19(3), 1335-1356, 2022.
- [33] Ince Z, Atakoglu OO, Yalcin MG. "Multivariate and Spatial Statistical Analysis of Geochemical Data of Dolomite: The Case of Industrial Raw Materials' Differentiation". *Montes Taurus Journal of Pure and Applied Mathematics*, 3(2), 1-21, 2021.
- [34] Yalcin MG, İlhan S. "Major and trace element geochemistry of Terra Rossa soil in the Kucukkoras region, Karaman, Turkey". *Geochemistry International*, 46(10), 1106-1121, 2008.
- [35] Yalcin MG, İlhan S. "Major and trace element geochemistry of bauxites of Ayranci, Karaman, central Bolkağ, Turkey". *Asian Journal of Chemistry*, 25(5), 2893-2904, 2013.
- [36] Yalcin MG, Setti M, Karakaya F, Sacchi E, İlbeyli N. "Geochemical and mineralogical characteristics of beach sediments along the coast between Alanya and Silifke (southern Turkey)". *Clay Minerals*, 50(2), 233-248, 2015.
- [37] Yalcin MG, Simsek G, Ocak SB, Yalcin F, Kalaycı Y, Karaman ME. "Multivariate statistics and heavy metals contamination in beach sediments from the Sakarya Canyon, Turkey". *Asian Journal of Chemistry*, 25(4), 2059-2066, 2013(b).
- [38] Kalaycı Ş. *SPSS Uygulamalı Çok Değişkenli İstatistik Teknikleri*. 2. Baskı. Ankara Türkiye, Asıl, 2010.

- [39] Ozer O, Yalcin MG. "Correlation of chemical contents of Sutlegen (Antalya) bauxites and regression analysis". *American Institute of Physics Conference Proceedings*, 2293(1), 18000-18004, 2020.
- [40] Yalcin MG, Narin I, Soylak M. "Heavy metal contents of the Karasu creek sediments, Nigde, Turkey". *Environmental Monitoring and Assessment*, 128(1), 351-357, 2007.
- [41] Yalcin MG, Tumuklu A, Sonmez M, Erdag DS. "Application of multivariate statistical approach to identify heavy metal sources in bottom soil of the Seyhan River (Adana), Turkey". *Environmental Monitoring and Assessment*, 164(1), 311-322, 2010.
- [42] Kaiser MO. "Kaiser-Meyer-Olkin measure for identity correlation matrix". *Journal of the Royal Statistical Society*, 52, 296-298, 1974.
- [43] Yalcin F. "Application of multivariate statistic and pollution index techniques to determine beach sand element distribution, East of Antalya City". *Filomat*, 34(2), 623-630, 2020a.
- [44] Yalcin F. "Data analysis of beach sands' chemical analysis using multivariate statistical methods and heavy metal distribution maps: the case of moonlight beach sands, Kemer, Antalya, Turkey". *Symmetry*, 12(9), 1-19, 2020(b).
- [45] Leventeli Y, Yalcin F. "Data analysis of heavy metal content in riverwater: multivariate statistical analysis and inequality expressions". *Journal of Inequalities and Applications*, 2021(1), 1-22, 2021.
- [46] Aydin B, Yalcin F, Ozer O, Yalcin MG. "Regression analysis and statistical examination of Knoop hardness on abrasion resistance in Lyca beige marbles". *Filomat*, 34(2), 609-614, 2020.
- [47] Sharma S. *Applied Multivariate Techniques*. 2nd ed. New York, USA, Wiley, 1996.
- [48] Yalcin F, Jonathan MP, Yalcin MG, Ilhan S, Leventeli Y. "Investigation of heavy metal content in beach sediments on the of Tasucu bay (Mersin) with geochemical and multivariate statistical approaches". *Journal of Engineering Sciences and Design*, 8(4), 1113-1125, 2020(a).
- [49] Yalcin MG, Ilhan S. "Major and trace element geochemistry of Terra Rossa soil in the Kucukkoras region, Karaman, Turkey". *Geochemistry International*, 46(10), 1106-1121, 2008.
- [50] Yalcin MG, Coskun B, Nyamsari DG, Yalcin F. "Geomedical, ecological risk, and statistical assessment of hazardous elements in shore sediments of the Iskenderun Gulf, Eastern Mediterranean, Turkey". *Environmental Earth Sciences*, 78(15), 1-28, 2019(b).
- [51] Yalcin MG. "Cluster analysis approach to identify metal sources in bottom sediments of Sultan Marsh canals, Turkey". *International Journal of Environment and Health*, 3(1), 106-125, 2009.
- [52] Yalcin MG, Battaloglu R. "Investigation of heavy metals pollution along the Nigde-Kayseri Road, Turkey". *Asian Journal of Chemistry*, 19 (3), 2257-2264, 2007.
- [53] Yalcin MG, Cevik O, Karaman ME. "Use of multivariate statistics methods to determine grain size, heavy metal distribution and origins of heavy metals in Mersin Bay (Eastern Mediterranean) coastal sediments". *Asian Journal of Chemistry*, 25(5), 2696-2702, 2013(a).
- [54] Yalcin F, Unal S, Yalcin MG, Akturk O, Ocak SB, Ozmen SF. "Investigation of the effect of hydrothermal waters on radionuclide activity concentrations in natural marble with multivariate statistical analysis". *Symmetry*, 12(8), 1-21, 2020(b).
- [55] Beauvais A, Colin F. "Formation and transformation processes of iron duricrust systems in tropical humid environment". *Chemical Geology*, 106(1), 77-101, 1993.
- [56] Bahlburg H, Dobrzinski N. "Chapter 6. A review of the Chemical Index of Alteration (CIA) and its application to the study of Neoproterozoic glacial deposits and climate transitions". *Geological Society*, 36, 81-92, 2011.
- [57] Fedo CM, Nesbitt HW, Young GM. "Unravelling the effects of potassium metasomatism in sedimentary rocks and paleosols, with implications for paleoweathering conditions and provenance". *Geology*, 23, 921-924, 1995.
- [58] Yalcin MG, Tumuklu A, Sonmez M, Erdag DS. "Application of multivariate statistical approach to identify heavy metal sources in bottom soil of the Seyhan River (Adana), Turkey". *Environmental Monitoring and Assessment*, 164(1), 311-322, 2010.
- [59] Matsubara H, Takashi ITO. "Simulation of three-dimensional chemical dissolution of limestone". *Pamukkale Üniversitesi Mühendislik Bilimleri Dergisi*, 26(8), 1393-1400, 2020.